Prototype Filter Optimization to Minimize Stopband Energy With NPR Constraint for Filter Bank Multicarrier Modulation Systems

Da Chen, Daiming Qu, Tao Jiang, *Senior Member, IEEE*, and Yejun He, *Senior Member, IEEE*

***Abstract*—Recently, filter bank multicarrier (FBMC) modulations have attracted increasing attention. The filter banks of FBMC are derived from a prototype filter that determines the system performance, such as stopband attenuation, intersymbol interference (ISI) and interchannel interference (ICI). In this paper, we formulate a problem of direct optimization of the filter impulse-response coefficients for the FBMC systems to minimize the stopband energy and constrain the ISI/ICI. Unfortunately, this filter optimization problem is nonconvex and highly nonlinear. Nevertheless, observing that all the functions in the optimization problem are twice-differentiable, we propose using the α-based Branch and Bound (αBB) algorithm to obtain the optimal solution. However, the convergence time of the algorithm is unacceptable because the number of unknowns (i.e., the filter coefficients) in the optimization problem is too large. The main contribution of this paper is that we propose a method to dramatically reduce the number of unknowns of the optimization problem through approximation of the constraints, so that the optimal solution of the approximated optimization problem can be obtained with acceptable computational complexity. Numerical results show that, the proposed approximation is reasonable, and the optimized filters obtained with the proposed method achieve significantly lower stopband energy than those with the frequency sampling and windowing based techniques.**

***Index Terms*—Filter bank multicarrier, offset quadrature amplitude modulation (OQAM), optimization, prototype filter, transmultiplexers.**

I. Introduction

MULTICARRIER MODULATIONS (MCM) have attracted a lot of attention due to the capability to efficiently cope with frequency selective channels. Much of the attention in the present literature emphasizes on the use of conventional orthogonal frequency division multiplexing (OFDM) [1]. However, the OFDM system uses rectangular pulse shaping on each subchannel, which leads to high out-of-band radiation. Moreover, the OFDM system sacrifices data transmission rate because of the insertion of cyclic prefix (CP). To remedy the problems of the OFDM systems, the filter bank multicarrier (FBMC) modulation has attracted increasing attention recently [2]–[8]. Compared with the conventional OFDM system, the FBMC system provides higher useful data rate because FBMC does not require the CP. Furthermore, it brings advantages such as robustness to narrow-band interference and lower sidelobes [9]. Recently, FBMC has been considered for the physical layer of cognitive radio systems [10].

FBMC techniques utilize filter-bank-based transmultiplexers (TMUXs) [11] to channelize the wide signal band. The filter banks of FBMC, consisting of synthesis and analysis filters, are typically derived from a prototype filter that determines the system performance, such as stopband attenuation, intersymbol interference (ISI) and interchannel interference (ICI). For the prototype filter design, it is often required that the stopband energy of the filter be minimized, while on the other hand, the nearly perfect reconstruction (NPR) condition be satisfied, i.e., the ISI/ICI resulted from the filters be kept lower than a certain threshold. There are also investigations on filters of perfect reconstruction (PR) condition [12], [13] and ISI-free filters in ISI channels [14], [15]. However, the cost of the PR condition and ISI-free property is the increase of stopband attenuation. In this paper, we focus on minimization of stopband energy, because lower stopband energy means better frequency selectivity. Excellent frequency selectivity is very important for wireless communication systems, especially for cognitive radio communication systems that rely on the filters for both data transmission and spectrum sensing [10].

The prototype filter optimization methods are categorized into three types in [16]: frequency sampling technique, windowing based technique, and direct optimization of filter coefficients. Frequency sampling techniques for prototype filter design were proposed in [17] and [18]. Different optimization criteria for the frequency sampling technique have been investigated in [16] and [19]. Windowing based techniques for the prototype filter design have been presented in [20]. With the frequency sampling and windowing based methods, prototype filter coefficients can be given using a closed-form representation that includes few adjustable design parameters. For example, the windowing based method optimizes the cut-off frequency and the weights of several cosine terms of the filter. On the contrary, direct optimization of prototype filter impulse-response coefficients aims at optimizing all the possible parameters that can affect the performance of the filter, thus

Manuscript received April 11, 2012; revised July 28, 2012 and September 24, 2012; accepted September 24, 2012. Date of publication October 03, 2012; date of current version December 12, 2012. The associate editor coordinating the review of this manuscript and approving it for publication was Dr. Ivan W. Selesnick. This work was supported in part by the National Science Foundation of China (No. 61271228 and 61172052), the Project-sponsored by SRF for ROCS, SEM, the National & Major Project (No. 2012ZX03003004), the Fundamental Research Funds for the Central Universities (HUST:2012TS019).

D. Chen, D. Qu, and T. Jiang are with Wuhan National Laboratory for Optoelectronics, Department of Electronics and Information Engineering, Huazhong University of Science and Technology, Wuhan, China (e-mail: chenda86@gmail.com; qudaiming@mail.hust.edu.cn; Tao.Jiang@ieee.org).

Y. He is with Department of Communication Engineering, College of Information Engineering, Shenzhen University, China (e-mail: heyejun@ieee.org).

Color versions of one or more of the figures in this paper are available online at http://ieeexplore.ieee.org.

Digital Object Identifier 10.1109/TSP.2012.2222397

has a potential to obtain better performance than the frequency sampling and windowing based methods. However, an evident drawback of this approach is that the number of unknowns (filter coefficients) increases dramatically when the number of subchannels grows high [21]. The general-purposed optimal FIR filter designs can be formulated as convex problems and be efficiently solved with some recent presented algorithms [22], [23]. However, when incorporated with the NPR condition, the problem of direct optimization of filter coefficients is often nonconvex and highly nonlinear, which is very sensitive to initial values and prohibited in practice due to high complexity. Moreover, the global optimality is not guaranteed, because the solution can be easily trapped in a local minimum [21], [24].

In this paper, we formulate a problem of direct optimization of the filter coefficients to both minimize the stopband energy and constrain the ISI/ICI for FBMC systems. Unfortunately, this filter optimization problem is nonconvex and highly nonlinear. Though the α-based Branch and Bound (αBB) algorithm can be employed to obtain the optimal solution in theory, the computational complexity is prohibited in practice since the number of unknowns (i.e., the filter coefficients) in the optimization problem is too large. The main contribution of this paper is that we propose a method to dramatically reduce the number of unknowns of the optimization problem through approximation of the constraints, so that the optimal solution of the approximated optimization problem can be obtained with acceptable computational complexity.

The rest of the paper is organized as follows. In Section II, a typical FBMC system, OFDM based on offset quadrature amplitude modulation (OFDM-OQAM), is described. In Section III, we formulate the optimization problem of prototype filter design and introduce the αBB algorithm, then, the number of variables of the optimization problem is reduced so that the convergence time of the αBB algorithm can be shortened to an acceptable interval. The numerical results are presented in Section IV. Finally, conclusions are summarized in Section V.

II. OFDM-OQAM System Model and ISI/ICI

In this section, we introduce the OFDM-OQAM system [5], [7] as an example of FBMC systems and present the expressions of the ISI/ICI for the OFDM-OQAM system.

A. OFDM-OQAM System Model

Fig. 1 presents the system model of the OFDM-OQAM system, which is equivalent to the TMUX model given in [7]. At the transmitter, the complex input symbols are written as

$$x_k(n) = a_k(n) + jb_k(n), \tag{1}$$

where $a_k(n)$ and $b_k(n)$ are the real and imaginary parts of the nth symbol on subcarrier k, respectively. The in-phase and quadrature components are staggered in time domain by $T/2$, where T is the symbol period. Then, the symbols are passed through a bank of transmission filters and modulated using N subcarrier modulators whose carrier frequencies are $1/T$-spaced apart. The OFDM-OQAM modulated signal is [25]

$$s(t) = \sum_{k=0}^{N-1} \sum_{n=-\infty}^{\infty} [a_k(n)h(t-nT) + jb_k(n)h(t-nT-T/2)]e^{jk\varphi_t}, \tag{2}$$

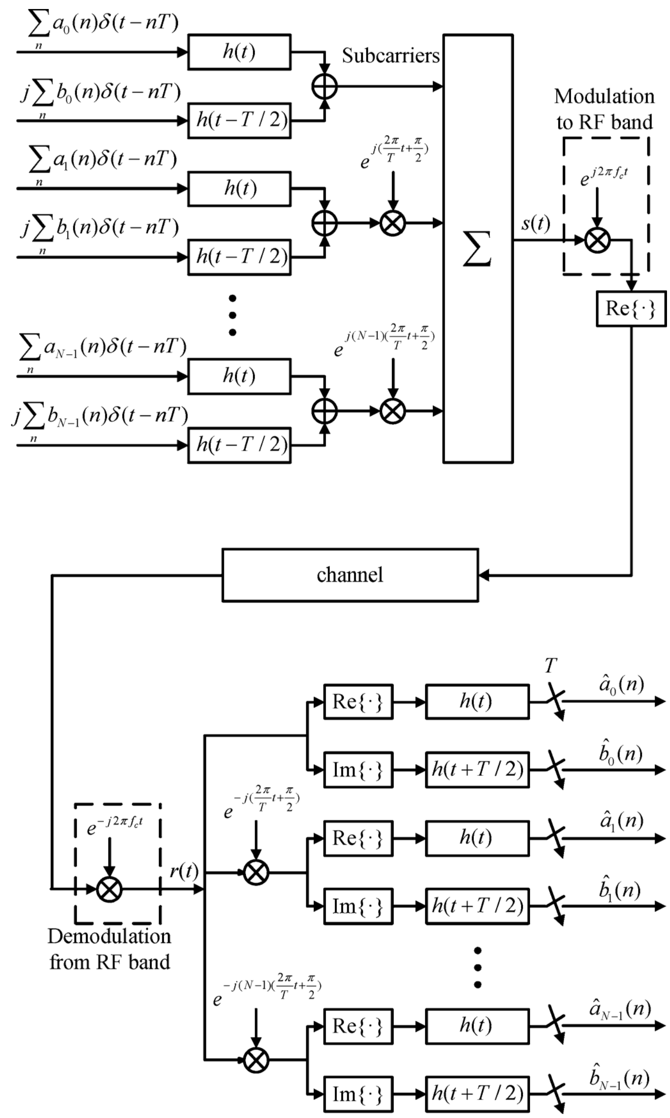

Fig. 1. OFDM-OQAM system model.

where $h(t)$ is the impulse response of the prototype filter and $\varphi_t = \frac{2\pi t}{T} + \frac{\pi}{2}$. After that, the OFDM-OQAM modulated signal $s(t)$ is modulated to RF band and transmitted.

For an ideal transmission system, the received signal at the receiver equals the transmitted signal at the transmitter. After demodulation from RF band, the received signal $r(t)$ is demodulated using N subcarrier demodulators and passed to a bank of matched filters. Then, the filtered signal is sampled with period T, and the output symbols are

$$\hat{x}_k(n) = \hat{a}_k(n) + j\hat{b}_k(n), \tag{3}$$

where $\hat{a}_k(n)$ and $\hat{b}_k(n)$ are the real and imaginary parts of the nth received symbol on subcarrier k, respectively. From [25], we have

$$\begin{aligned}\hat{a}_k(n) = &\sum_{n'=-\infty}^{\infty} \sum_{k'=0}^{N-1} \int_{-\infty}^{\infty} h(nT-t) \\ &\times \{a_{k'}(n')h(t-n'T)\cos[(k'-k)\varphi_t] \\ &-b_{k'}(n')h(t-n'T-T/2)\sin[(k'-k)\varphi_t]\}dt, \end{aligned}\tag{4}$$

and

$$\hat{b}_k(n) = \sum_{n'=-\infty}^{\infty} \sum_{k'=0}^{N-1} \int_{-\infty}^{\infty} h(nT - t + T/2) \times \{a_{k'}(n')h(t-n'T)\sin[(k'-k)\varphi_t] + b_{k'}(n')h(t-n'T-T/2)\cos[(k'-k)\varphi_t]\}dt. \quad (5)$$

If the prototype filter satisfies the PR condition, which is illustrated as

$$\int_{-\infty}^{+\infty} h(t-n'T)h(nT-t)\cos[(k'-k)\varphi_t]dt = \delta(k'-k, n'-n), \quad (6)$$

$$\int_{-\infty}^{+\infty} h(t-n'T-T/2)h(nT-t)\sin[(k'-k)\varphi_t]dt = 0, \quad (7)$$

$$\int_{-\infty}^{+\infty} h(t-n'T)h(nT-t+T/2)\sin[(k'-k)\varphi_t]dt = 0, \quad (8)$$

$$\int_{-\infty}^{+\infty} h(t-n'T-T/2)h(nT-t+T/2)\cos[(k'-k)\varphi_t]dt = \delta(k'-k, n'-n), \quad (9)$$

the output at the receiver equals the input at the transmitter [25], i.e.,

$$\hat{x}_k(n) = x_k(n). \quad (10)$$

Obviously, we can constrain $h(t)$ to be real and even so that (7) and (8) are automatically satisfied [25].

B. ISI/ICI in the OFDM-OQAM System

A prototype filter could be designed to fulfill PR conditions or to provide NPR characteristics. The PR conditions are not essential because the PR property is obtained only with an ideal transmission channel and interferences generated from the filter bank structure with NPR are small enough compared with the interferences due to nonideal transmission channel. Moreover, NPR designs are more efficient, e.g., providing lower stopband energy with the same filter length of PR designs.

Denote the ISI/ICI interference to $a_k(n)$ and $b_k(n)$ by $I^a_{k,n}$ and $I^b_{k,n}$, respectively. The expected power of the interference are

$$\begin{aligned}\text{Power}(I^a_{k,n}) &= \text{E}[(\hat{a}_k(n) - a_k(n))^2] \\ &= \text{E}\left[\left(\sum_{n'=-\infty}^{\infty} \sum_{k'=0}^{N-1} \int_{-\infty}^{\infty} h(nT-t) \times \{a_{k'}(n')h(t-n'T)\cos[(k'-k)\varphi_t] - b_{k'}(n')h(t-n'T-T/2)\sin[(k'-k)\varphi_t]\}dt - a_k(n)\right)^2\right] \\ &= \text{E}\left[\left(\sum_{n'=-\infty}^{\infty} \sum_{k'=0}^{N-1} I^a_{k,n,k',n'} - a_k(n)\right)^2\right], \quad (11)\end{aligned}$$

$$\begin{aligned}\text{Power}(I^b_{k,n}) &= \text{E}\left[(\hat{b}_k(n) - b_k(n))^2\right] \\ &= \text{E}\left[\left(\sum_{n'=-\infty}^{\infty} \sum_{k'=0}^{N-1} I^b_{k,n,k',n'} - b_k(n)\right)^2\right], \quad (12)\end{aligned}$$

respectively, where $I^a_{k,n,k',n'}$ represents the contribution of $x_{k'}(n')$ to $\hat{a}_k(n)$ and $I^b_{k,n,k',n'}$ represents the contribution of $x_{k'}(n')$ to $\hat{b}_k(n)$. According to (4), the contribution of $x_{k'}(n')$ to $\hat{a}_k(n)$ is

$$I^a_{k,n,k',n'} = a_{k'}(n')C'_{k,n,k',n'} - b_{k'}(n')C''_{k,n,k',n'}, \quad (13)$$

where

$$C'_{k,n,k',n'} = \int_{-\infty}^{\infty} h(nT-t)h(t-n'T)\cos[(k'-k)\varphi_t]dt, \quad (14)$$

$$C''_{k,n,k',n'} = \int_{-\infty}^{\infty} h(nT-t)h(t-n'T-\frac{T}{2})\sin[(k'-k)\varphi_t]dt. \quad (15)$$

To design the filter in the discrete time domain, we replace $h(t)$ with its discrete time version $h(l), l = 0, 1, \ldots, L_p - 1$, for (14) and (15), where $h(l)$ corresponds to the filter impulse response at time lT/N and L_p represents the length of the discrete time filter. (Note that we abuse the notation $h(\cdot)$ for both the continuous and discrete time domain filter in this paper, and it represents the discrete time domain filter in the rest of this paper.) Then, the discrete time expressions of (14) and (15) are

$$C'_{k,n,k',n'} = \sum_{l=0}^{L_p-1} \{h(nN-l)h(l-n'N) \times \cos[(k'-k)(2\pi l/TN + \pi/2)]\}, \quad (16)$$

$$C''_{k,n,k',n'} = \sum_{l=0}^{L_p-1} \{h(nN-l)h(l-n'N-N/2) \times \sin[(k'-k)(2\pi l/TN + \pi/2)]\}, \quad (17)$$

respectively.

The distributions of $a_{k'}(n')$ and $b_{k'}(n')$ have unit power and are symmetric to the origin due to randomness of the information bits, i.e.,

$$\text{E}[(a_{k'}(n'))^2] = \text{E}[(b_{k'}(n'))^2] = 1. \quad (18)$$

$$\text{E}[a_{k'}(n')] = \text{E}[b_{k'}(n')] = 0, \quad (19)$$

Moreover, the distributions of $a_{k'}(n')$ and $b_{k'}(n')$ are independent. Then, from (13), (18) and (19), the expectation of the power of $I^a_{k,n,k',n'}$ is given as

$$\begin{aligned}\text{E}[(I^a_{k,n,k',n'})^2] &= (C'_{k,n,k',n'})^2\text{E}[(a_{k'}(n'))^2] + (C''_{k,n,k',n'})^2\text{E}[(b_{k'}(n'))^2] \\ &\quad - 2C'_{k,n,k',n'}C''_{k,n,k',n'}\text{E}[a_{k'}(n')]\text{E}[b_{k'}(n')] \\ &= (C'_{k,n,k',n'})^2 + (C''_{k,n,k',n'})^2. \quad (20)\end{aligned}$$

By evaluating (16) and (17) with $(k',n') = (k,n)$, we have $C'_{k,n,k,n} = \sum_{l=0}^{L_p-1}(h(l))^2$ and $C''_{k,n,k,n} = 0$. Therefore, $I^a_{k,n,k,n}$, the contribution of $x_k(n)$ to $\hat{a}_k(n)$, is

$$I^a_{k,n,k,n} = a_k(n)C'_{k,n,k,n} - b_k(n)C''_{k,n,k,n} = a_k(n)\sum_{l=0}^{L_p-1}(h(l))^2. \quad (21)$$

Apparently, it should be satisfied that

$$\sum_{l=0}^{L_p-1}(h(l))^2 = 1, \quad (22)$$

and

$$I^a_{k,n,k,n} = a_k(n). \quad (23)$$

Noticing that the distributions of $a_{k'}(n')$ and $b_{k'}(n')$ are independent for different (k',n'), the expected power of the ISI/ICI interference to $a_k(n)$ is calculated as

$$\begin{aligned}\mathrm{Power}(I^a_{k,n}) &= \mathrm{E}\left[\left(\sum_{n'=-\infty}^{\infty}\sum_{k'=0}^{N-1} I^a_{k,n,k',n'} - a_k(n)\right)^2\right] \\ &= \sum_{n'=-\infty}^{\infty}\left\{\sum_{k'=0,(k',n')\neq(k,n)}^{N-1} \mathrm{E}\left[(I^a_{k,n,k',n'})^2\right]\right\} \\ &\quad + \mathrm{E}\left[\left(I^a_{k,n,k,n} - a_k(n)\right)^2\right] \\ &= \sum_{n'=-\infty}^{\infty}\left\{\sum_{k'=0,(k',n')\neq(k,n)}^{N-1} \mathrm{E}\left[\left(I^a_{k,n,k',n'}\right)^2\right]\right\}. \end{aligned} \quad (24)$$

The expected power of the ISI/ICI interference to $b_k(n)$, $\mathrm{Power}(I^b_{k,n})$, can be similarly calculated, and it was found to be equal to $\mathrm{Power}(I^a_{k,n})$. The strict proof is very tedious, therefore we only give a brief description of the major steps of the proof in the followings.

We transform (5) as

$$\begin{aligned}\hat{b}_k(n) = \sum_{k'=0}^{N-1}\int_{-\infty}^{\infty} & h(nT - t + T/2) \\ \times \Bigg\{ & \sum_{n'=-\infty}^{\infty} b_{k'}(n')h(t - n'T - T/2)\cos[(k'-k)\varphi_t] \\ & + \sum_{n'=-\infty}^{\infty} a_{k'}(n')h(t - n'T)\sin[(k'-k)\varphi_t]\Bigg\}dt. \end{aligned} \quad (25)$$

Noticing that the summation over n' is from $-\infty$ to ∞, we can replace n' with $n'+1$ in the second summation in braces and (25) becomes

$$\begin{aligned}\hat{b}_k(n) = \sum_{k'=0}^{N-1}\int_{-\infty}^{\infty} & h(nT - t + T/2) \\ \times \Bigg\{ & \sum_{n'=-\infty}^{\infty} b_{k'}(n')h(t - n'T - T/2)\cos[(k'-k)\varphi_t] \\ & + \sum_{n'=-\infty}^{\infty} a_{k'}(n'+1)h(t - n'T - T) \\ & \times \sin[(k'-k)\varphi_t]\Bigg\}dt. \end{aligned} \quad (26)$$

The integral over t is also from $-\infty$ to ∞. Then, we can replace t with $t + T/2$ in (26) and

$$\begin{aligned}\hat{b}_k(n) = \sum_{n'=-\infty}^{\infty}\sum_{k'=0}^{N-1}\int_{-\infty}^{\infty} & h(nT - t) \\ & \times \{b_{k'}(n')h(t - n'T)\cos[(k'-k)\varphi_{t+T/2}] \\ & + a_{k'}(n'+1)h(t - n'T - T/2) \\ & \times \sin[(k'-k)\varphi_{t+T/2}]\}dt. \end{aligned} \quad (27)$$

Since $\varphi_{t+T/2} = \frac{2\pi(t+T/2)}{T} + \frac{\pi}{2} = \varphi_t + \pi$, (27) can be rewritten as

$$\begin{aligned}\hat{b}_k(n) = \sum_{n'=-\infty}^{\infty}\sum_{k'=0}^{N-1}\int_{-\infty}^{\infty} & h(nT - t) \\ & \times \{(-1)^{k'-k}b_{k'}(n')h(t - n'T)\cos[(k'-k)\varphi_t] \\ & + (-1)^{k'-k}a_{k'}(n'+1)h(t - n'T - T/2) \\ & \times \sin[(k'-k)\varphi_t]\}dt. \end{aligned} \quad (28)$$

It is observed that the expressions of (28) and (4) are almost the same, except for the term of $(-1)^{k'-k}$ and the exchange of positions of $b_k(n)$ and $a_k(n)$. Exploit this symmetry and follow the steps of (12) to (24), it is easy to derive that $\mathrm{Power}(I^b_{k,n}) = \mathrm{Power}(I^a_{k,n})$.

It is easy to prove that $\mathrm{Power}(I^a_{k,n})$ and $\mathrm{Power}(I^b_{k,n})$ are independent of k and n if all the symbols in time and frequency domain are independent and identically distributed. Then, the level of total ISI/ICI of an OFDM-OQAM system can be measured by $\mathrm{Power}(I^a_{k,n})$ and $\mathrm{Power}(I^b_{k,n})$ with any choice of k and n.

III. Direct Optimization of the Filter Coefficients

In this section, we formulate the problem of direct optimization of the filter coefficients. Then, we attempt to solve the optimization problem with the αBB algorithm and reduced number of variables.

A. Problem Formulation and the αBB Algorithm

We make the filter $h(l)$ an even and real NPR filter with the length L_p. Then, $h(l)$ should satisfy

$$h(l) = h(L_p - 1 - l), l = 0, 1, \ldots, L_p - 1. \quad (29)$$

The Fourier transform of the designed filter $h(l)$ is

$$H(e^{jw}) = \sum_{l=0}^{L_p-1} h(l)e^{-jwl}. \quad (30)$$

Then, the magnitude response of the filter $h(l)$ is

$$|H(e^{jw})| = \left| \sum_{l=0}^{L_p-1} h(l)e^{-jwl} \right|. \tag{31}$$

In this paper, the optimization objective is to minimize the stopband energy of the prototype filter, where the stopband region is denoted by $[w_0, \pi]$. With the constraint of (22) and constraint of the ISI/ICI power, the filter design problem can be written as an optimization problem:

$$\mathbf{P}1: \quad \min_{h(0),h(1),\ldots,h(L_p-1)} \int_{w_0}^{\pi} |H(e^{jw})|^2 dw, \tag{32a}$$

$$\text{subject to} \quad h(l) = h(L_p-1-l), l = 0, 1, \ldots, L_p-1, \tag{32b}$$

$$\text{Power}(I^a_{k,n}) \le \text{TH}, \tag{32c}$$

$$\text{Power}(I^b_{k,n}) \le \text{TH}, \tag{32d}$$

$$\sum_{l=0}^{L_p-1} (h(l))^2 = 1, \tag{32e}$$

where a low threshold TH guarantees that the error between the input at the transmitter and the output at the receiver is small enough so that the designed filter is an NPR filter. Since $\text{Power}(I^a_{k,n}) = \text{Power}(I^b_{k,n})$, the constraint (32d) can be removed.

The constraint (32e) can be relaxed as

$$\sum_{l=0}^{L_p-1} (h(l))^2 \ge 1. \tag{33}$$

The reason is that if $[h'(0), h'(1), \ldots, h'(L_p-1)]$ is the optimal solution of $\mathbf{P}1$ with the relaxed constraint, it must have $\sum_{l=0}^{L_p-1} (h'(l))^2 = 1$. To prove this, assume that $h'(l)$ satisfies $\sum_{l=0}^{L_p-1} (h'(l))^2 = a^2 > 1$. Then, it is direct to verify that $h^*(l) = \frac{1}{a}h'(l)$ satisfies (32b) to (32d), and (33). However, the objective value (32a) for $h^*(l)$ is smaller, which contradicts the fact that $h'(l)$ is the optimal solution.

Moreover, we could control the stopband attenuation within specified frequency ranges by adding weights to the objective function (32a), i.e., the optimization problem $\mathbf{P}1$ is modified as

$$\mathbf{P}2: \quad \min_{h(0),h(1),\ldots,h(L_p-1)} \int_{w_0}^{\pi} W(w)|H(e^{jw})|^2 dw, \tag{34a}$$

$$\text{subject to} \quad h(l) = h(L_p-1-l), l = 0, 1, \ldots, L_p-1, \tag{34b}$$

$$\text{Power}(I^a_{k,n}) \le \text{TH}, \tag{34c}$$

$$\sum_{l=0}^{L_p-1} (h(l))^2 \ge 1, \tag{34d}$$

where $W(w) > 0$ is the weight of frequency w.

Furthermore, according to (34b), only half of the variables are independent. Thus, let

$$\mathbf{x} = [x_1, x_2, \ldots, x_L]^{\mathrm{T}} = \begin{cases} \left[h(0), h(1), \ldots, h\left(\frac{L_p}{2}-1\right)\right]^{\mathrm{T}}, & \text{if } L_p \text{ is even}, \\ \left[h(0), h(1), \ldots, h\left(\frac{L_p-1}{2}\right)\right]^{\mathrm{T}}, & \text{if } L_p \text{ is odd}. \end{cases} \tag{35}$$

Then, the optimization problem $\mathbf{P}2$ can be rewritten as

$$\mathbf{P}3: \quad \min_{\mathbf{x}} f_0(\mathbf{x}) = \int_{w_0}^{\pi} W(w)|H(e^{jw})|^2 dw, \tag{36a}$$

$$\text{subject to} \quad f_1(\mathbf{x}) = \text{Power}(I^a_{k,n}) - \text{TH} \le 0, \tag{36b}$$

$$f_2(\mathbf{x}) = -\left(\sum_{l=0}^{L_p-1} (h(l))^2 - 1\right) \le 0. \tag{36c}$$

Unfortunately, the problem $\mathbf{P}3$ is nonconvex due to (36b) and (36c). Nevertheless, all the functions in $\mathbf{P}3$ are twice-differentiable and the so called αBB algorithm is applicable to this kind of problem.

The αBB algorithm offers mathematical guarantees for convergence to a point arbitrarily close to the global minimum for the large class of twice-differentiable nonlinear programming problems (NLPs). The key idea is to construct a converging sequence of upper and lower bounds on the global minimum through the convex relaxation of the original problem [26]–[28]. The detailed process of the αBB algorithm is described in [27].

Though the optimization problem can be solved optimally by the αBB algorithm in theory, the convergence time is too long to be acceptable in practice. Since the convergence time increases exponentially with the number of variables (i.e., the filter coefficients) in the optimization, the main purpose of the following subsections is to reduce the number of variables.

B. Variable Transformation

The objective function (36a) is a convex quadratic function, which can be written in vector form as $f_0(\mathbf{x}) = \mathbf{x}^{\mathrm{T}}\mathbf{C}\mathbf{x}$, where $\mathbf{C}$ is a real symmetric positive-definite matrix. We denote the ith row and jth column element of $\mathbf{C}$ by c_{ij}, then, $f_0(\mathbf{x})$ can be expressed as

$$\begin{aligned} f_0(\mathbf{x}) = \mathbf{x}^{\mathrm{T}}\mathbf{C}\mathbf{x} &= \sum_{i=1}^{L}\sum_{j=1}^{L} c_{ij}x_ix_j \\ &= \int_{w_0}^{\pi} W(w)|H(e^{jw})|^2 dw \\ &= \int_{w_0}^{\pi} W(w)\left|\sum_{l=0}^{L_p-1} h(l)e^{-jwl}\right|^2 dw \\ &= \int_{w_0}^{\pi} W(w)\left\{\left(\sum_{l=0}^{L_p-1} h(l)\cos(wl)\right)^2 \right. \\ &\quad \left. + \left(\sum_{l=0}^{L_p-1} h(l)\sin(wl)\right)^2\right\} dw. \end{aligned} \tag{37}$$

By setting x_i equal to 1 and all other variables equal to 0, we easily obtain c_{ii} as

$$c_{ii} = f_0(\mathbf{x} = [0, \ldots, x_i = 1, 0, \ldots, 0]^{\mathrm{T}}), \quad i = 1, 2, \ldots L. \tag{38}$$

Similarly, $c_{ij} (i \ne j)$ can be obtained by setting x_i, x_j equal to 1 and all other variables equal to 0, i.e.,

$$\begin{aligned} c_{ij} = 1/2 \times \{f_0(\mathbf{x} = [0, \ldots, x_i = 1, 0, \ldots, \\ x_j = 1, 0, \ldots, 0]^{\mathrm{T}}) - c_{ii} - c_{jj}\}, \\ i, j = 1, 2, \ldots L, i \ne j. \end{aligned} \tag{39}$$

Utilizing (35), (37), (38) and (39), we can easily calculate the values of c_{ii} and $c_{ij} (i \neq j)$.

Since $\mathbf{C}$ is a real symmetric matrix, we can always find L positive eigenvalues $\lambda_1, \lambda_2, \ldots, \lambda_L$ in ascending order $(0 < \lambda_1 \leq \lambda_2 \leq \cdots \leq \lambda_L)$ and the corresponding orthonormal eigenvectors $\mathbf{v}_1, \mathbf{v}_2, \ldots, \mathbf{v}_L$ (column vectors) for $\mathbf{C}$. Then, we apply an orthonormal transformation

$$\mathbf{x} = \mathbf{V}\mathbf{y}, \tag{40}$$

where $\mathbf{V} = [\mathbf{v}_1, \mathbf{v}_2, \ldots, \mathbf{v}_L]$ is the transformation matrix and $\mathbf{y} = [y_1, y_2, \ldots, y_L]^{\mathrm{T}}$ denotes the transformed variables. With the linear transformation, $f_0(\mathbf{x})$ is written as

$$\begin{aligned} f_0(\mathbf{x}) &= \mathbf{x}^{\mathrm{T}}\mathbf{C}\mathbf{x} = \mathbf{y}^{\mathrm{T}}\mathrm{Diag}(\lambda_1, \lambda_2, \ldots, \lambda_L)\mathbf{y} \\ &= \lambda_1 y_1^2 + \lambda_2 y_2^2 + \ldots + \lambda_L y_L^2, \end{aligned} \tag{41}$$

where $\mathrm{Diag}(\,\cdot\,)$ denotes a diagonal matrix. Let

$$g_0(\mathbf{y}) = \lambda_1 y_1^2 + \lambda_2 y_2^2 + \ldots + \lambda_L y_L^2 = f_0(\mathbf{x}). \tag{42}$$

We also perform the linear transformation on the constraints (36b)-(36c) and let

$$g_i(\mathbf{y}) = f_i(\mathbf{x}), i = 1, 2. \tag{43}$$

Then, the optimization problem $\mathbf{P}3$ can be rewritten as

$$\begin{aligned} \mathbf{P}4 : \min_{\mathbf{y}} \quad & g_0(\mathbf{y}), \\ \text{subject to} \quad & g_i(\mathbf{y}) \leq 0,\ i = 1, 2. \end{aligned} \tag{44}$$

C. Determination of Search Region With a Feasible Solution

In this subsection, we aim to determine the search region for each variable with the help of a known feasible solution of problem $\mathbf{P}4$.

The filter obtained using the frequency sampling technique in [18] is a feasible solution that satisfies all constraints of (32), as long as TH is not set to be too small. The impulse response coefficients of the filter are given as

$$\begin{aligned} h(l) = P(0) + 2\sum_{i=1}^{Q-1}(-1)^i P(i)\cos\left(\frac{2\pi i}{QN}(l+1)\right), \\ l = 0, 1, \ldots, QN-2, \end{aligned} \tag{45}$$

where $QN - 1$ is the length of the filter and $P(i)$ are coefficients dependent on Q. For $Q = 3$, $P(0) = 1$, $P(1) = 0.91143783$, $P(2) = 0.41143783$; for $Q = 4$, $P(0) = 1$, $P(1) = 0.97195983$, $P(2) = 0.70710678$, $P(3) = 0.23514695$.

Let $\mathbf{y}_0$ denote the vector of transformed variables that represents the filter obtained using the frequency sampling technique. Since $\mathbf{y}_0$ is a feasible solution of the problem $\mathbf{P}4$, the optimal solution $\mathbf{y}^*$ must satisfy

$$\lambda_1(y_1^*)^2 + \lambda_2(y_2^*)^2 + \cdots + \lambda_L(y_L^*)^2 = g_0(\mathbf{y}^*) \leq g_0(\mathbf{y}_0). \tag{46}$$

This means that the search region of the optimal solution can be greatly reduced with the knowledge of the feasible solution $\mathbf{y}_0$, i.e., the optimization problem $\mathbf{P}4$ becomes

$$\begin{aligned} \mathbf{P}5 : \min_{\mathbf{y}} \quad & g_0(\mathbf{y}), \\ \text{subject to} \quad & g_i(\mathbf{y}) \leq 0, i = 1, 2, \\ & \lambda_1 y_1^2 + \lambda_2 y_2^2 + \ldots + \lambda_L y_L^2 \leq g_0(\mathbf{y}_0). \end{aligned} \tag{47}$$

The newly added constraint infers that

$$\begin{aligned} &\lambda_j(y_j^*)^2 \leq \lambda_1(y_1^*)^2 + \lambda_2(y_2^*)^2 + \ldots + \lambda_L(y_L^*)^2 \leq g_0(\mathbf{y}_0) \\ &\quad\Longrightarrow \sqrt{\lambda_i}|y_j^*| \leq \sqrt{g_0(\mathbf{y}_0)} \\ &\quad\Longrightarrow -\sqrt{\frac{g_0(\mathbf{y}_0)}{\lambda_j}} \leq y_j^* \leq \sqrt{\frac{g_0(\mathbf{y}_0)}{\lambda_i}},\ j = 1, 2, \ldots, L. \end{aligned} \tag{48}$$

We use the above box constraint as the initial set for the αBB algorithm.

D. Reduction of the Variable Number Through Approximation of the Constraints

According to (48), the variable y_j with larger λ_j is constrained to be smaller. For λ_j large enough, the variable y_j is so little that it may be neglected for the constraints $g_i(\mathbf{y}), i = 1, 2$. Thus, we conjecture that it is a good approximation for all constraints $g_i(\mathbf{y})$ that the variables corresponding to the smaller eigenvalues are preserved while the variables corresponding to the larger eigenvalues are set to zero.

For each variable vector $\mathbf{y} = [y_1, y_2, \ldots, y_L]$, we form a new vector $\mathbf{y}'$ of length L, where $\mathbf{y}' = [y_1, y_2, \ldots, y_{L'}, 0, \ldots, 0]$. If L' is large enough, we have the following approximation of the constraints

$$g_i(\mathbf{y}) \approx g_i(\mathbf{y}'),\ i = 1, 2. \tag{49}$$

The approximation in (49) and determination of L' will be discussed in the following subsection. Using the above approximation of the constraints, the optimization problem $\mathbf{P}5$ can be approximated as

$$\mathbf{P6} : \min_{\mathbf{y}} \quad g_0(\mathbf{y}) = \left\{\sum_{j=1}^{L'}\lambda_j y_j^2 + \sum_{j=L'+1}^{L}\lambda_j y_j^2\right\}, \tag{50a}$$
$$\text{subject to} \quad g_i(\mathbf{y}') \leq 0,\ i = 1, 2, \tag{50b}$$
$$\sum_{j=1}^{L}\lambda_j y_j^2 \leq g_0(\mathbf{y}_0). \tag{50c}$$

Next, we consider the optimization problem that relaxes (50c) of $\mathbf{P6}$:

$$\mathbf{P7} : \min_{\mathbf{y}} \quad g_0(\mathbf{y}) = \left\{\sum_{j=1}^{L'}\lambda_j y_j^2 + \sum_{j=L'+1}^{L}\lambda_j y_j^2\right\}, \tag{51a}$$
$$\text{subject to} \quad g_i(\mathbf{y}') \leq 0, i = 1, 2, \tag{51b}$$
$$\sum_{j=1}^{L'}\lambda_j y_j^2 \leq g_0(\mathbf{y}_0). \tag{51c}$$

Let $\mathbf{y}^\dagger$ denote the optimal solution of the problem $\mathbf{P}7$. Since $y_{L'+1}, \ldots, y_L$ are not present in the constraints and $\sum_{j=L'+1}^{L} \lambda_j y_j^2 \geq 0$, the optimal solution of $\mathbf{P}7$ must satisfy that $y_{L'+1}^\dagger = \ldots = y_L^\dagger = 0$. Therefore, $\mathbf{y}^\dagger$ satisfies (50c) and it is a feasible solution of the problem $\mathbf{P}6$, which means that $g_0(\mathbf{y}^\dagger) \geq g_0(\mathbf{y}^*)$, where $\mathbf{y}^*$ is the optimal solution of $\mathbf{P}6$. On the other hand, (51c) is a relaxation of (50c), which means that $g_0(\mathbf{y}^\dagger) \leq g_0(\mathbf{y}^*)$. Therefore, it is clear that $g_0(\mathbf{y}^\dagger) = g_0(\mathbf{y}^*)$, which means that optimal solution of $\mathbf{P}7$ is also the optimal solution of $\mathbf{P}6$, and $y_{L'+1}^* = \ldots = y_L^* = 0$.

Finally, $y_1^\dagger, \ldots, y_{L'}^\dagger (y_1^*, \ldots, y_{L'}^*)$ can be obtained by solving the following problem, which is derived from $\mathbf{P}7$ by removing the zero variables $y_{L'+1}, \ldots, y_L$,

$$\begin{aligned} \mathbf{P}8: \min_{y_1,\ldots,y_{L'}} \quad & \sum_{j=1}^{L'} \lambda_j y_j^2, \\ \text{subject to} \quad & g_i(y_1, \ldots, y_{L'}, 0, \ldots, 0) \leq 0, i = 1, 2, \\ & \sum_{j=1}^{L'} \lambda_j y_j^2 \leq g_0(\mathbf{y}_0). \end{aligned} \tag{52}$$

The problem $\mathbf{P}8$ can be efficiently solved by the αBB algorithm if L' is very small. In the next section, we will show that L' is indeed very small.

E. Verification of the Approximation of the Constraints

To verify that the approximation of (49) is good for a certain L', we can increase L' gradually and solve $\mathbf{P}8$ for each L'. If the resulted objective value stops decreasing (or the decrease is negligible) for a certain L' and above, the approximation of preserving this certain number of variables is good enough. The detail will be discussed in the next section.

As another way to verify that the approximation of (49) is reasonable for a certain L', we can compute the maximum difference $d_i(L')$ between $g_i(\mathbf{y})$ and $g_i(\mathbf{y}')$ over the search region of $\mathbf{P}5$, for $i = 1, 2$, respectively. This leads to the following optimization problem:

$$\begin{aligned} d_i(L') = \max_{\mathbf{y}} & |g_i(\mathbf{y}) - g_i(\mathbf{y}')|, \ i = 1, 2 \\ \text{subject to} \quad & g_1(\mathbf{y}) \leq 0, g_2(\mathbf{y}) \leq 0, \\ & \sum_{j=1}^{L} \lambda_j y_j^2 \leq g_0(\mathbf{y}_0). \end{aligned} \tag{53}$$

Since $d_i(L')$ is the maximum difference between constraints $g_i(\mathbf{y})$ and $g_i(\mathbf{y}')$, and $g_i(\mathbf{y}) \leq 0$ is meant to satisfy the NPR condition, approximating $g_i(\mathbf{y})$ with $g_i(\mathbf{y}')$ is reasonable as long as $d_1(L') \ll \mathrm{TH}$ and $d_2(L') \ll 1$.

In order to make (53) smooth, we could transform (53) into two optimization problem, i.e.,

$$\begin{aligned} d_i^+(L') = \max_{\mathbf{y}} & (g_i(\mathbf{y}) - g_i(\mathbf{y}')), \ i = 1, 2, \\ & \text{subject to constraints of (53),} \end{aligned} \tag{54}$$

and

$$\begin{aligned} d_i^-(L') = \max_{\mathbf{y}} & (g_i(\mathbf{y}') - g_i(\mathbf{y})), \ i = 1, 2, \\ & \text{subject to constraints of (53).} \end{aligned} \tag{55}$$

Then, $d_i(L') = \max(d_i^+(L'), d_i^-(L'))$.

Note that, solving the problem (53) is as difficult as the solving of $\mathbf{P}5$. However, suboptimal solutions of (53), which are available by applying heuristic algorithms, reflect the magnitude order of $d_i(L')$ and can be used as approximations of $d_i(L')$. One suboptimal algorithm we tried is sequential quadratic programming (SQP). Since the solution obtained by the SQP algorithm is highly dependent on the initial variables, we apply the SQP algorithm [30] to (54) and (55) multiple times (1000 times in the computations of the next section) with random initial variables within the search region, and use the maximum result to approximate $d_i(L')$.

There have been investigations on sparse filter design [31]. If a low complexity convex relaxation of the ISI/ICI constraint is available, the method proposed in [31] can be employed for the problem of reducing the variable number.

IV. Numerical Results

In this section, numerical computations are conducted to determine the appropriate number of preserved variables, and verify the effectiveness of the proposed algorithm. We set the ISI/ICI threshold $\mathrm{TH} = 10^{-3}$ and 10^{-4}, the number of subcarriers $N = 64$ and 256, and the filter length $L_p = 3N - 1$ and $4N - 1$ for the optimization problem. The weight $W(w)$ is set to be 1 for the computations of Figs. 3, 4 and 7, where the optimization objective is to minimize the stopband energy within $[w_0, \pi] = [2\pi/N, \pi]$. $W(w)$ is varied for Figs. 5 and 6, where the optimization objective is to control the stopband attenuation within specified frequency ranges.

By solving the problem (53) with the SQP algorithm, within a range of L', we obtain the corresponding $d_i(L')$ for $i = 1, 2$, respectively. For the SQP algorithm, we run the algorithm 1000 times with random initial variables within the search region, and use the maximum result to approximate $d_i(L')$. In Fig. 2, approximated $d_i(L')$ versus L' for $\mathrm{TH} = 10^{-4}$, $L_p = 4N - 1$ and $N = 256$ are depicted. It is observed that $d_i(L')$ for $i = 1, 2$ are sufficiently small when $L' \geq 3$, i.e., $d_1(3) \ll \mathrm{TH}$ and $d_2(3) \ll 1$. To verify that the approximation of (49) is good for $L' = 3$, we increase L' gradually and solve $\mathbf{P}8$ for each L'. From Table I, it is observed that the resulted objective value almost stops decreasing for $L' = 3$ and above, which verifies that the approximation of (49) is good for $L' = 3$. Similar results are obtained for other combinations of parameters. Therefore, we set $L' = 3$ in the following computations.

For the αBB algorithm to solve $\mathbf{P}8$, we stop the iteration when the differences between the lower bounds of the remaining subsets and the minimum upper bound are within 0.5×10^{-11}. The computation was performed by a MATLAB program running on a desktop computer equipped with an Intel i5-2400 3.1 GHz CPU. The convergence time for the αBB algorithm with $\mathrm{TH} = 10^{-4}$, $L_p = 4N - 1$ and $N = 256$ is about 1803 seconds, which is acceptable considering that the design procedure is needed to be performed only once for typical communication systems.

To verify the performance advantage of the proposed filters, we compare them with three types of filters listed below:

1) Original frequency sampling filters: filters obtained in [18], which are denoted by $h_1(l)$. We are interested in this comparison because it is concluded in [21] that it is very hard to find better solution than the filters obtained with the frequency sampling technique.

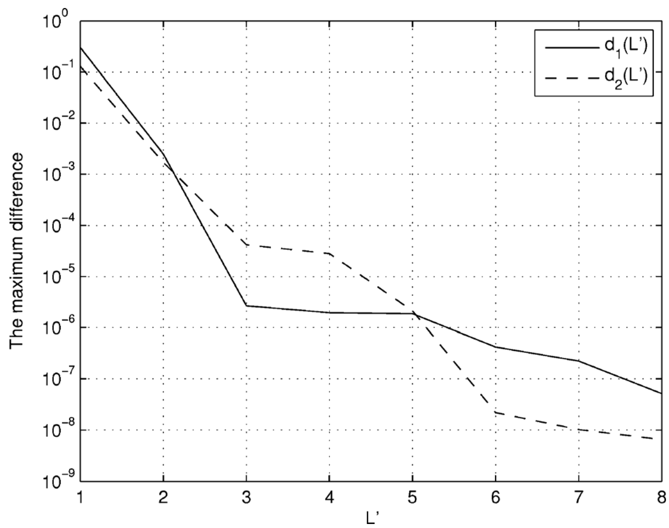

Fig. 2. The approximated $d_i(L')$ for $\mathrm{TH} = 10^{-4}$, $L_p = 4N - 1$ with $N = 256$, $i = 1, 2$.

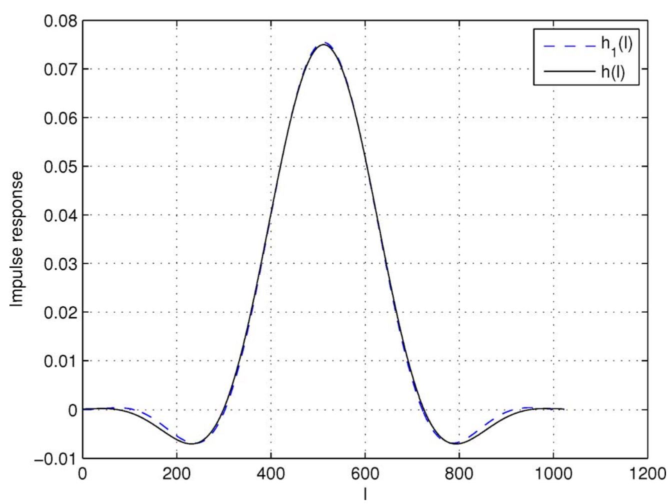

Fig. 3. The impulse responses of $h(l)$ and $h_1(l)$ with $\mathrm{TH} = 10^{-4}$, $N = 256$ and $L_p = 4N - 1$.

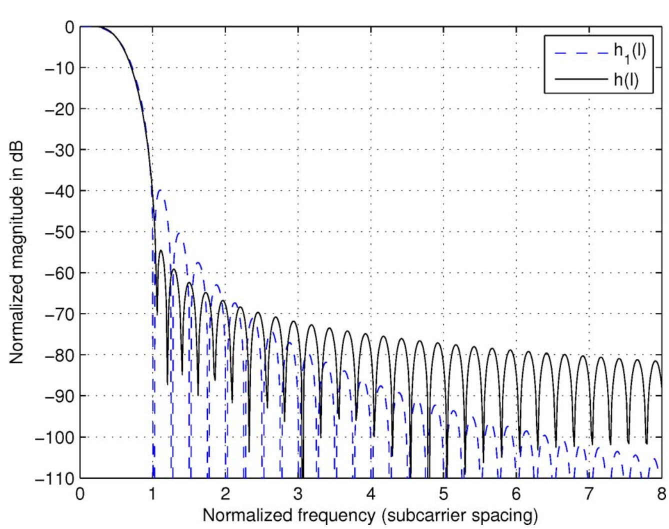

Fig. 4. The normalized magnitude responses of $h(l)$ and $h_1(l)$ with $\mathrm{TH} = 10^{-4}$, $N = 256$ and $L_p = 4N - 1$.

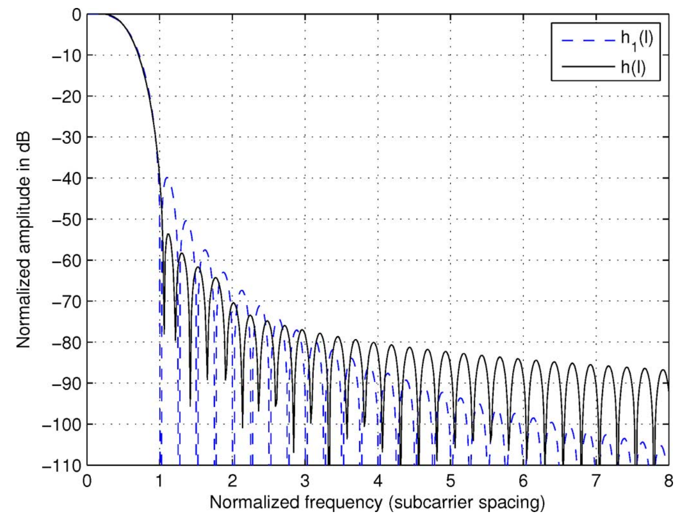

Fig. 5. The normalized magnitude responses of $h_1(l)$ and $h(l)$ with $W(w) = W_1(w)$, $\mathrm{TH} = 10^{-4}$, $N = 256$ and $L_p = 4N - 1$.

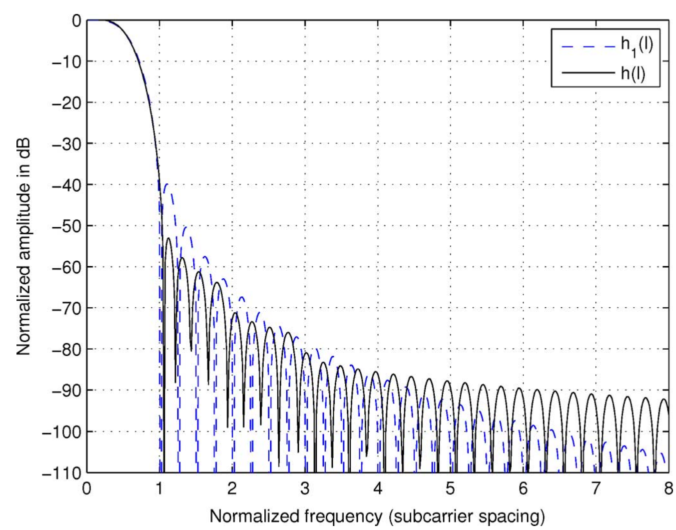

Fig. 6. The normalized magnitude responses of $h_1(l)$ and $h(l)$ with $W(w) = W_2(w)$, $\mathrm{TH} = 10^{-4}$, $N = 256$ and $L_p = 4N - 1$.

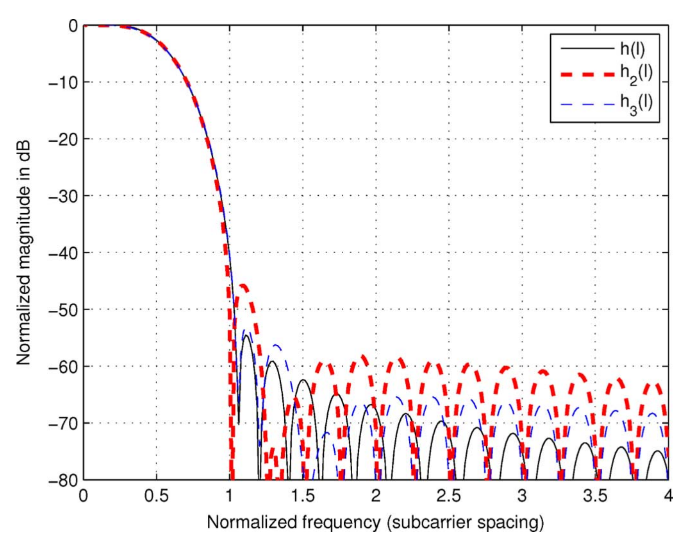

Fig. 7. The normalized magnitude responses of $h(l)$, $h_2(l)$ and $h_3(l)$ with $\mathrm{TH} = 10^{-4}$, $N = 256$ and $L_p = 4N - 1$.

TABLE I
THE OBJECTIVE VALUES OF THE OPTIMIZED FILTERS $h(l)$ WITH $\mathrm{TH} = 10^{-4}$, $N = 256$, $L_p = 4N - 1$ AND VARIED L'

Filter	L'	Objective value
$h(l)$	3	2.402×10^{-8} (-76.1943dB)
	4	2.398×10^{-8} (-76.2015dB)
	5	2.398×10^{-8} (-76.2015dB)
	6	2.398×10^{-8} (-76.2015dB)
	7	2.397×10^{-8} (-76.2033dB)
	8	2.397×10^{-8} (-76.2033dB)

2) Optimized frequency sampling filters: optimized filters using the frequency sampling based technique (optimized with the same objective and constraints as those of $\mathbf{P}1$), which are denoted by $h_2(l)$. The frequency sampling based filter is expressed as [16]

$$h_2(l) = P(0) + 2\sum_{i=1}^{Q-1}(-1)^i P(i)\cos\left(\frac{2\pi i}{QN}(l+1)\right), \quad l = 0, 1, \ldots, QN-2, \tag{56}$$

where $P(i), i = 0, \ldots, Q-1$ are adjustable coefficients. We substitute $h_2(l)$ into the optimization problem $\mathbf{P}1$ and solve $\mathbf{P}1$ to obtain the optimized filter. For $L_p = 3N-1$, Q is set to 3, then $P(0) = 1$, $P(2) = \sqrt{1 - P(1)^2}$. For $L_p = 4N - 1$, Q is set to 4, then $P(0) = 1, P(2) = \sqrt{2}/2$, $P(3) = \sqrt{1 - P(1)^2}$. Therefore, only one parameter, $P(1)$, is required to be optimized for both cases. The optimized frequency sampling filter is obtained by optimizing $P(1)$ with the same objective and constraints as those of $\mathbf{P}1$.

3) Optimized windowing based filters: optimized filters using the windowing based technique (optimized with the same objective and constraints as those of $\mathbf{P}1$), which are denoted by $h_3(l)$. The windowing based filter is expressed as [20]

$$h_3(l) = w(l)h_c(l), \tag{57}$$

where $h_c(l)$ is given as

$$h_c(l) = \frac{\sin[w_c(l - (L_p-1)/2)]}{\pi(l - (L_p-1)/2)}, \quad l = 0, 1, \ldots, L_p - 1, \tag{58}$$

and $w(l)$ is given as

$$w(l) = \sum_{i=0}^{3}(-1)^i A_i \cos\left(\frac{2\pi i l}{L_p - 1}\right). \tag{59}$$

The optimized windowing based filter is obtained by optimizing the cut-off frequency w_c and four weights $A(i), i = 0, 1, 2, 3$, with the same objective and constraints as those of $\mathbf{P}1$.

The impulse responses of $h(l)$ and $h_1(l)$ with $\mathrm{TH} = 10^{-4}$, $N = 256$ and $L_p = 4N - 1$ are presented in Fig. 3 as an example. Noticeable differences between the proposed filter and the corresponding filter obtained with the frequency sampling technique in [18] can be observed from the figure. Fig. 4 shows the normalized magnitude responses of $h(l)$ and $h_1(l)$. It is observed from Fig. 4 that the sidelobes of $h(l)$ within the normalized frequency range between Subcarrier 1 and Subcarrier 2, which dominate the overall stopband energy, are significantly lower than those of $h_1(l)$.

For some applications, it is needed to further lower the sidelobes in certain frequency range. To satisfy this requirement, one can adjust the weights $W(w)$ in the optimization problem. In Fig. 5, we obtain the optimized filter $h(l)$ with $\mathrm{TH} = 10^{-4}$, $N = 256$, $L_p = 4N - 1$ and

$$W(w) = W_1(w) = \begin{cases} 1, & w_0 \le w < 2w_0 \\ 4, & 2w_0 \le w \le \pi \end{cases} \tag{60}$$

It is shown that the sidelobes of $h(l)$ with $W_1(w)$ within Subcarrier 1 and 3 are lower than those of $h_1(l)$ with $\mathrm{TH} = 10^{-4}$, $N = 256$ and $L_p = 4N - 1$. In Fig. 6, we obtain the optimized filter $h(l)$ with

$$W(w) = W_2(w) = \begin{cases} 1, & w_0 \le w < 2w_0 \\ 4, & 2w_0 \le w < 3w_0 \\ 15, & 3w_0 \le w \le \pi \end{cases} \tag{61}$$

It is shown that the sidelobes of $h(l)$ with $W_2(w)$ within the Subcarrier 1 and 4 are lower than those of $h_1(l)$ with $\mathrm{TH} = 10^{-4}$, $N = 256$ and $L_p = 4N - 1$. These examples show that the sidelobes of the designed filters within specified frequency ranges can be delicately controlled by adjusting the weights in the optimization formulation, so that it is lower than those of the filters obtained by using the frequency sampling technique.

In the computation of Fig. 7, we solve the optimization problem of $\mathbf{P}1$ using the frequency sampling and windowing based techniques, and compare the resulted filters with the proposed filters, for $\mathrm{TH} = 10^{-4}$, $N = 256$ and $L_p = 4N - 1$. The objective value of $h_2(l)$ and $h_3(l)$ is 1.2502×10^{-7} (-69.0302 dB) and 4.028×10^{-8} (-73.9487 dB), respectively, which are both greater than the objective value of the proposed filter $h(l)$, 2.402×10^{-8} (-76.1941 dB). The reason that our proposed method achieves the best objective is: the proposed method is a reasonable approximation of the direct optimization of all filter coefficients, while the other two methods only optimize few parameters of the filter.

In Table II, the objective values of the proposed filters $h(l)$ with different combinations of parameters are compared with those of the original frequency sampling filters $h_1(l)$, the optimized frequency sampling filters $h_2(l)$ and the optimized windowing based filters $h_3(l)$, respectively. It is observed that the objective values (which represent the overall stopband energy) of the proposed filters $h(l)$ are significantly lower than those of the corresponding filters for comparison. In average, the objective values of the proposed filters $h(l)$ are 12.0341 dB lower than the original frequency sampling filters $h_1(l)$, 7.9751 dB lower than the optimized frequency sampling filters $h_2(l)$ and 3.3970 dB lower than the optimized windowing based filters $h_3(l)$. Particularly, when TH and L_p are larger ($\mathrm{TH} = 10^{-3}$ and $L_p = 4N - 1$), the performance gain of the proposed filters $h(l)$ over other three filters is larger: in average, the objective values of the proposed filters $h(l)$ are 17.6170 dB lower than the original frequency sampling filters $h_1(l)$, 13.3343 dB lower

TABLE II
THE OBJECTIVE VALUES OF THE OPTIMIZED FILTERS $h(l)$ AND FILTERS $h_1(l)$, $h_2(l)$, $h_3(l)$ FOR COMPARISON

Parameters	Filter	Objective value
$\mathrm{TH}=10^{-4}$ $N=64$ $L_p=3N-1$	$h(l)$	1.19320×10^{-6} (-59.2329dB)
	$h_1(l)$	1.005929×10^{-5} (-49.9743dB)
	$h_2(l)$	4.18962×10^{-6} (-53.7783dB)
	$h_3(l)$	1.80235×10^{-6} (-57.4416dB)
$\mathrm{TH}=10^{-4}$ $N=64$ $L_p=4N-1$	$h(l)$	9.963×10^{-8} (-70.0161dB)
	$h_1(l)$	1.34760×10^{-6} (-58.7044dB)
	$h_2(l)$	5.0528×10^{-7} (-62.9647dB)
	$h_3(l)$	1.7139×10^{-7} (-67.6601dB)
$\mathrm{TH}=10^{-4}$ $N=256$ $L_p=3N-1$	$h(l)$	2.8281×10^{-7} (-65.4851dB)
	$h_1(l)$	2.51483×10^{-6} (-55.9949dB)
	$h_2(l)$	1.03242×10^{-6} (-59.8614dB)
	$h_3(l)$	4.1726×10^{-7} (-63.7959dB)
$\mathrm{TH}=10^{-4}$ $N=256$ $L_p=4N-1$	$h(l)$	2.402×10^{-8} (-76.1943dB)
	$h_1(l)$	3.3690×10^{-7} (-64.7250dB)
	$h_2(l)$	1.2502×10^{-7} (-69.0302dB)
	$h_3(l)$	4.028×10^{-8} (-73.9491dB)
$\mathrm{TH}=10^{-3}$ $N=64$ $L_p=3N-1$	$h(l)$	1.09290×10^{-6} (-59.6142dB)
	$h_1(l)$	1.005929×10^{-5} (-49.9743dB)
	$h_2(l)$	4.18962×10^{-6} (-53.7783dB)
	$h_3(l)$	1.80235×10^{-6} (-57.4416dB)
$\mathrm{TH}=10^{-3}$ $N=64$ $L_p=4N-1$	$h(l)$	2.339×10^{-8} (-76.3097dB)
	$h_1(l)$	1.34760×10^{-6} (-58.7044dB)
	$h_2(l)$	5.0528×10^{-7} (-62.9647dB)
	$h_3(l)$	1.3472×10^{-7} (-68.7057dB)
$\mathrm{TH}=10^{-3}$ $N=256$ $L_p=3N-1$	$h(l)$	2.5917×10^{-7} (-65.8642dB)
	$h_1(l)$	2.51483×10^{-6} (-55.9949dB)
	$h_2(l)$	1.03242×10^{-6} (-59.8614dB)
	$h_3(l)$	4.0676×10^{-7} (-63.9066dB)
$\mathrm{TH}=10^{-3}$ $N=256$ $L_p=4N-1$	$h(l)$	5.816×10^{-9} (-82.3538dB)
	$h_1(l)$	3.3690×10^{-7} (-64.7250dB)
	$h_2(l)$	1.2502×10^{-7} (-69.0302dB)
	$h_3(l)$	3.167×10^{-8} (-74.9935dB)

than the optimized frequency sampling filters $h_2(l)$ and 7.4822 dB lower than the optimized windowing based filters $h_3(l)$.

To verify that the optimized filters $h(l)$, $h_2(l)$ and $h_3(l)$ conform to the ISI/ICI requirements, we simulate a pair of directly connected OFDM-OQAM transmitter and receiver with the designed filters and compute the mean squared error (MSE) between the transmitted symbols and received symbols. The transmitted signals are 4QAM modulated, and $\mathrm{TH}=10^{-4}$, $N=256$, $L_p=4N-1$ or $3N-1$. The MSEs with $h_1(l)$, $h_2(l)$ and $h_3(l)$ are also presented as comparison. Table III shows that the MSEs with the optimized filters are all successfully constrained within the predefined $\mathrm{TH}=10^{-4}$, thus it can be concluded that the optimized filters satisfy the NPR property. Similar simulations for the optimized filters with other combinations of parameters are also performed. The results also show that the MSEs with the optimized filters are all successfully constrained within the predefined TH.

TABLE III
MSE BETWEEN THE TRANSMITTED SYMBOLS AND THE RECEIVED SYMBOLS WITH $\mathrm{TH}=10^{-4}$ AND $N=256$

Parameters	Filter	MSE (real part)	MSE (imaginary part)
$\mathrm{TH}=10^{-4}$ $N=256$ $L_p=3N-1$	$h(l)$	9.9759×10^{-5}	1.0095×10^{-4}
	$h_1(l)$	4.5362×10^{-5}	4.6218×10^{-5}
	$h_2(l)$	6.5610×10^{-5}	6.5031×10^{-5}
	$h_3(l)$	9.9804×10^{-5}	9.9989×10^{-5}
$\mathrm{TH}=10^{-4}$ $N=256$ $L_p=4N-1$	$h(l)$	1.0187×10^{-4}	1.0003×10^{-4}
	$h_1(l)$	3.0172×10^{-7}	3.0255×10^{-7}
	$h_2(l)$	1.6159×10^{-6}	1.6304×10^{-6}
	$h_3(l)$	1.0160×10^{-4}	9.9791×10^{-5}

V. CONCLUSION

In this paper, we have formulated a problem of direct optimization of the filter coefficients to both minimize the stopband energy and constrain the ISI/ICI for FBMC systems. We proposed to employ the α-based Branch and Bound (αBB) algorithm to obtain the optimal solution, and proposed a method to dramatically reduce the number of unknowns of the optimization problem through approximation of the constraints. Numerical results show that the proposed approximation is reasonable, and the optimized filters obtained with the proposed method achieve significantly lower stopband energy than those with the frequency sampling and windowing based techniques.

REFERENCES

[1] J. A. C. Bingham, "Multicarrier modulation for data transmission: An idea whose time has come," *IEEE Commun. Mag.*, vol. 28, no. 5, pp. 5–14, May 1990.

[2] R. W. Chang, "Synthesis of band-limited orthogonal signals for multichannel data transmission," *Bell. Syst. Tech. J.*, vol. 45, no. 10, pp. 1775–1796, Dec. 1966.

[3] B. R. Saltzberg, "Performance of an efficient parallel data transmission system," *IEEE Trans. Commun. Technol.*, vol. 15, no. 6, pp. 805–811, Feb. 1967.

[4] B. Hirosaki, "An orthogonally multiplexed QAM system using the discrete Fourier transform," *IEEE Trans. Commun.*, vol. 29, no. 7, pp. 982–989, Jul. 1981.

[5] B. L. Floch, M. Alard, and C. Berrou, "Coded orthogonal frequency division multiplex," *Proc. IEEE*, vol. 83, no. 6, pp. 982–996, June 1995.

[6] K. W. Martin, "Small sidelobe filter design for multitone data-communication applications," *IEEE Trans. Circuits Syst. II*, vol. 45, no. 8, pp. 1155–1161, Aug. 1998.

[7] P. Siohan, C. Siclet, and N. Lacaille, "Analysis and design of OFDM/OQAM systems based on filterbank theory," *IEEE Trans. Signal Process.*, vol. 50, no. 5, pp. 1170–1183, May 2002.

[8] H. Boelcskei, "Orthogonal frequency division multiplexing based on offset QAM," in *Advances in Gabor Analysis*. Boston, MA: Birkhaüser, 2003, pp. 321–352.

[9] M. Bellanger, "Physical layer for future broadband radio systems," in *Proc. Radio Wireless Symp. Conf.*, New Orleans, LA, Jan. 10–14, 2010, pp. 835–838.

[10] B. Farhang-Boroujeny and R. Kempter, "Multicarrier communication techniques for spectrum sensing and communication in cognitive radios," *IEEE Commun. Mag.*, vol. 46, no. 4, pp. 80–85, Apr. 2008.

[11] P. P. Vaidyanathan, *Multirate Systems and Filter Banks*. Englewood Cliffs, NJ: Prentice-Hall, 1993.

[12] Z. Cvetkovic and M. Vetterli, "Tight Weyl-Heisenberg frames in $\ell^2(\mathbf{Z})$," *IEEE Trans. Signal Process.*, vol. 46, no. 5, pp. 1256–1259, May 1998.

[13] F. D. Beaulieu and B. Champagne, "Multicarrier modulation using perfect reconstruction DFT filter bank transceivers," in *Proc. 5th Int. Conf. Inf., Commun., Signal Process.*, Bangkok, Thailand, Dec. 6–9, 2005, pp. 111–115.

[14] A. Scaglione, G. B. Giannakis, and S. Barbarossa, "Redundant filterbank precoders and equalizers. I. Unification and optimal designs," *IEEE Trans. Signal Process.*, vol. 47, no. 7, pp. 1988–2006, Jul. 1999.

[15] S.-M. Phoong, Y. Chang, and C.-Y. Chen, "DFT-modulated filterbank transceivers for multipath fading channels," *IEEE Trans. Signal Process.*, vol. 53, no. 1, pp. 182–192, Jan. 2005.

[16] A. Viholainen, T. Ihalainen, T. H. Stitz, M. Renfors, and M. Bellanger, "Prototype filter design for filter bank based multicarrier transmission," in *Proc. 17th Eur. Signal Process. Conf.*, Glasgow, Scotland, Aug. 24–28, 2009, pp. 1359–1363.

[17] M. G. Bellanger, "Specification and design of a prototype filter for filter bank based multicarrier transmission," in *Proc. IEEE Int. Conf. Acoust., Speech, Signal Process.*, Salt Lake City, UT, May 7–11, 2001, pp. 2417–2420.

[18] S. Mirabbasi and K. Martin, "Overlapped complex-modulated transmultiplexer filters with simplified design and superior stopbands," *IEEE Trans. Circuits Syst. II, Analog Digit. Signal Process.*, vol. 50, no. 8, pp. 456–469, Aug. 2003.

[19] F. Cruz-Roldan, C. Heneghan, J. B. Saez-Landete, M. Blanco-Velasco, and P. Amo-Lopez, "Multi-objective optimisation technique to design digital filters for modulated multi-rate systems," *Electron. Lett.*, vol. 44, no. 13, pp. 827–828, Jun. 2008.

[20] P. Martin-Martin, R. Bregovic, A. Martin-Marcos, F. Cruz-Roldan, and T. Saramaki, "A generalized window approach for designing transmultiplexers," *IEEE Trans. Circuits Syst. I, Reg. Papers*, vol. 55, no. 9, pp. 2696–2706, Oct. 2008.

[21] A. Viholainen, M. Bellanger, and M. Huchard, "Prototype filter and structure optimization," [Online]. Available: http://www.ict-phydyas.org/delivrables/PHYDYAS-D5-1.pdf/view

[22] X. Lai, "Optimal design of nonlinear-phase FIR filters with prescribed phase error," *IEEE Trans. Signal Process.*, vol. 57, no. 9, pp. 3399–3410, Sep. 2009.

[23] T. Davidson, "Enriching the art of FIR filter design via convex optimization," *IEEE Signal Process. Mag.*, vol. 27, no. 3, pp. 89–101, May 2010.

[24] D. Chen, D. Qu, and T. Jiang, "Novel prototype filter design for FBMC based cognitive radio systems through direct optimization of filter coefficients," presented at the Int. Conf. Wireless Commun. Signal Process., Suzhou, China, Oct. 21–23, 2010.

[25] P. Amini, R. Kempter, and B. Farhang-Boroujeny, "A comparison of alternative filterbank multicarrier methods in cognitive radio systems," presented at the Softw. Defined Radio Tech. Conf., Orlando, FL, Nov. 13–16, 2006.

[26] I. P. Androulakis, C. D. Maranas, and C. A. Floudas, "αBB: A global optimization method for general constrained nonconvex problems," *J. Global Optim.*, vol. 7, no. 4, pp. 337–343, Dec. 1995.

[27] C. S. Adjiman, S. Dallwig, C. A. Floudas, and A. Neumaier, "A global optimization method, αBB, for general twice-differentiable constrained NLPs—I. Theoretical advances," *Comput. Chem. Eng.*, vol. 22, no. 9, pp. 1137–1158, Aug. 1998.

[28] C. S. Adjiman, I. P. Androulakis, and C. A. Floudas, "A global optimization method, αBB, for general twice-differentiable constrained NLPs—II. Implementation and computational results," *Comput. Chem. Eng.*, vol. 22, no. 9, pp. 1159–1179, Aug. 1998.

[29] C. D. Maranas and C. A. Floudas, "Global minimum potential energy conformations of small molecules," *J. Global Optim.*, vol. 4, no. 2, pp. 135–170, Mar. 1994.

[30] J. Hu, Z. Wu, H. McCann, L. E. Davis, and C. Xie, "Sequential quadratic programming method for solution of electromagnetic inverse problems," *IEEE Trans. Antennas Propag.*, vol. 53, no. 8, pp. 2680–2687, Aug. 2005.

[31] D. Wei, "Design of discrete-time filters for efficient implementation," Ph.D. dissertation, Electr. Eng. Comput. Sci. Dept., Mass. Inst. of Technol., Cambridge, MA, 2011.

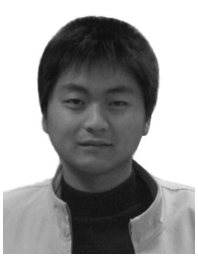

Da Chen received the B.S. degree from Huazhong University of Science and Technology, Wuhan, China, in 2009. He is currently working towards the Ph.D. degree at Huazhong University of Science and Technology.

His current research interests include the areas of wireless communications, especially for FBMC systems with emphasis on research of filter design.

Daiming Qu received the Ph.D. degree in information and communication engineering from Huazhong University of Science and Technology, Wuhan, China, in 2003.

He is currently an Associate Professor in the Department of Electronics and Information Engineering, Huazhong University of Science and Technology. His current research interests include signal processing, coding, and dynamic spectrum techniques for wireless communications.

Tao Jiang (M'06–SM'10) received the B.S. and M.S. degrees in applied geophysics from China University of Geosciences, Wuhan, China, in 1997 and 2000, respectively, and the Ph.D. degree in information and communication engineering from Huazhong University of Science and Technology, Wuhan, China, in 2004.

From August 2004 to December 2007, he worked in such universities as Brunel University and the University of Michigan in the U.K. and the U.S., respectively. He is currently a Full Professor in Wuhan National Laboratory for Optoelectronics, Department of Electronics and Information Engineering, Huazhong University of Science and Technology, Wuhan, China. He has authored or coauthored over 100 technical papers in major journals and conferences and five books/chapters in the areas of communications. His current research interests include the areas of wireless communications and corresponding signal processing, especially for cognitive wireless access, vehicular technology, OFDM, UWB and MIMO, cooperative networks, smart grid, and wireless sensor networks.

Dr. Jiang served or is serving as symposium technical program committee member of many major IEEE conferences, including INFOCOM, ICC, and GLOBECOM. He is invited to serve as TPC Symposium Chair for the IEEE GLOBECOM 2013 and IEEEE WCNC 2013, and as a General Co-Chair for the workshop of M2M Communications and Networking in conjunction with IEEE INFOCOM 2011. He served or is serving as Associate Editor of some technical journals in communications, including the *IEEE Communications Surveys and Tutorials* and the IEEE TRANSACTIONS ON VEHICULAR TECHNOLOGY. He is a recipient of the Best Paper Awards in IEEE CHINACOM 2009 and WCSP 2009. He is a Member of the IEEE Communication Society, the IEEE Vehicular Technology Society, the IEEE Broadcasting Society, the IEEE Signal Processing Society, and the IEEE Circuits and Systems Society.

Yejun He (SM'09) received the Ph.D. degree in information and communication engineering from Huazhong University of Science and Technology (HUST), Wuhan, China, in 2005.

He is currently a Professor of Information and Communication Engineering at Shenzhen University, China. His research interests include channel coding and modulation; MIMO-OFDM wireless communication; space-time processing; and smart antennas. He is the principal investigator in more than ten current or finished research projects, including NSFC of China. He translated three English books into Chinese and authored or coauthored more than 60 research papers as well as applied for 11 patents since 2002.

Dr. He is a senior member of the China Institute of Communications and China Institute of Electronics as well as a member of the Youth Committee of the China Institute of Communications. He is also serving or has served as reviewer/Technical Program Committee member/Session Chair for various journals and conferences, including the IEEE TRANSACTIONS ON VEHICULAR TECHNOLOGY, the IEEE COMMUNICATIONS LETTERS, the *International Journal of Communication Systems*, and *Wireless Communications and Mobile Computing*, and has been Associate Editor of *Security and Communication Networks* since 2012. He served as the Organizing Committee Vice-Chair of CMC 2010 and an Editor of the CMC 2010 Proceedings. He acted as the publicity chair of IEEE PIMRC 2012.